AIP | Proceedings

LWFA with Low Energy Raman Seeded Pulses

Mykhailo Fomyts'kyi, Charles Chiu, Michael Downer, and Franklin Grigsby

Articles you may be interested in

Relativistic Extension of the Accelerating-Focusing Phase in 3D Nonlinear Laser Wake
AIP Conf. Proc. **877**, 735 (2006); 10.1063/1.2409209

Expanded Model Predictions for Seeded SM-LWFA and Pseudo-Resonant LWFA
AIP Conf. Proc. **877**, 714 (2006); 10.1063/1.2409206

Laser wakefield acceleration by petawatt ultrashort laser pulses
AIP Conf. Proc. **737**, 757 (2004); 10.1063/1.1842619

Development of 873 nm Raman Seed Pulse for Raman-seeded Laser Wakefield
Acceleration
AIP Conf. Proc. **737**, 559 (2004); 10.1063/1.1842591

High-Energy Electron Beam Generation by a Laser Pulse Propagating in a Plasma
AIP Conf. Proc. **647**, 710 (2002); 10.1063/1.1524926

LWFA with Low Energy Raman Seeded Pulses

Mykhailo Fomyts'kyi[*], Charles Chiu[*], Michael Downer[*] and Franklin Grigsby[*]

[*]*FOCUS Center and Institute for Fusion Studies*
University of Texas at Austin
Austin, Texas 78712

Abstract. Analytical and numerical calculations of plasma wakefield excitation and particle acceleration by Raman seeded laser pulse in self-modulation regime are presented. We derive energy threshold for self-modulation of diffraction-limited pulses. The parameter range where the Raman seeded amplitude plays an important role is investigated. We show that the seeded amplitude provides a coherent control mechanism for the phase of the wakefield wave. We show that with the use of Raman seed self-modulated wakefield acceleration is achievable for the pulses of intensities much lower than those typically used in the experiments. In particular, our 2D particle-in-cell simulations show that 30 mJ pulse combined with Raman seeded pulse, which is 1% in intensity of the main pulse is capable of generating ∼1 nC of relativistic electrons.

1. INTRODUCTION

Of the various methods of driving large-amplitude plasma waves [1], the Self-Modulated Laser Wakefield Accelerator (SM-LWFA) [2, 3, 4] has so far yielded electron bunches of the highest energy (tails to >200 MeV [5, 6]), charge (> 1 nC/bunch [7, 8]) and collimation (transverse emittance $\varepsilon_\perp < 0.1\pi$ mm · mrad [9]). The beam properties achieved are favorable enough that near-term applications of the SM-LWFA - including table-top nuclear activation of rare isotopes [8], injectors for conventional high-energy physics accelerators, and radiation oncology [10, 11, 12] - are gradually emerging.

A disadvantage of the SM-LWFA is the high peak power of the driving laser pulses, which is required to achieve the necessary beam energy, collimation, and peak current for practical applications. This restricts laser repetition rate to a few Hertz, and average current to nano-amp levels. Most demonstrations of SM-LWFA have, in fact, been essentially single-shot (≪ 1 Hz) [13, 14, 7, 15]. Only recently has high quality SM-LWFA been achieved at repetition rates as high as 10 Hz [6, 8]. However, kilohertz repetition rates (micro-amp average currents) are desirable for most applications. Recently laser systems capable of delivering pulses approaching ∼1 TW at ∼1 kHz repetition rate have indeed been developed [16]. However, these pulses currently fall short of the threshold required for efficient SM-LWFA. Therefore, it is timely to investigate schemes for "seeding" the growth of RMI that have the potential to reduce the threshold energy for SM-LWFA to levels achievable by kHz laser systems, while retaining the favorable beam characteristics (high peak current, collimation, energy).

Here we investigate through 1D and 2D particle-in-cell (PIC) simulations a Raman-seeding mechanism [17, 18, 19], in which a driving pulse with frequency ω is "seeded"

by a co-propagating superposed pulse of a substantially lower intensity and with a frequency $\omega_{seed} \approx \omega - \omega_p$. The presence of this seed pulse greatly enhances RMI compared to the unseeded case. Recent demonstration of experimental schemes for generating Raman-shifted seed pulses by chirped-pulse stimulated Raman scattering in Raman-active crystals [20] has further motivated the present study.

2. RESONANCE MODULATION INSTABILITY AND SEEDING

2.1. 1D and 3D regimes of the modulation

There are several different regimes of Resonance Modulational Instability (RMI) [21, 22]. When $16(\omega/\omega_p)^2/(k_p\sigma_\perp)^2 < 1$, where $k_p = \omega_p/c$, $\sigma_\perp$ is the spotsize, the modulation is caused by 1D RMI known as Forward Raman Scattering (FRS). When $\sigma_\perp k_p < \omega/\omega_p$, the problem becomes essentially three-dimensional and the dominant modulation mechanism is Envelope Self-Modulation (ESM). For the parameters of interest (low energy pulses with the interaction length limited by diffraction or dephasing), the 4-wave FRS and ESM are important. For the detailed classification of RMI regimes, see Ref. [21].

At early times, the main mechanism of the pulse modulation in the self-modulation regime is FRS [22, 23]. The time-special growth of the wakefield $\chi = \delta n/n_0 - a_0^2/4$ associated with 4-wave Raman instability before saturation can be described by [23]:

$$\chi_s = \chi_{s0} \sum_{n=0}^{\infty} \left(\frac{\psi/c}{t - \psi/c} \right)^n I_{2n}(\Gamma) \rightarrow \chi_{s0} \frac{\exp\Gamma}{\sqrt{2\pi\Gamma}}, \tag{1}$$

where the gain

$$\Gamma_{1D1} = \frac{a_0}{2} \frac{\omega_p^2}{\omega_0} \sqrt{(t - \psi/c)\psi/c} \tag{2}$$

is the number of the e-fold magnifications of the original perturbation χ_{s0}, n_0 is the plasma density, δn is the plasma density perturbation, $a_0 = eA/mc^2$ is the normalized vector potential, t is the interaction time during which the laser pulse passes through the gas jet, and ψ is the distance from the head of the pulse. The last expression is the asymptotic form for large values of Γ.

For pulses of small spotsize 3D ESMI quickly becomes dominant [21, 22]. The growth of the modulation can be characterized by the corresponding gain:

$$\Gamma_{3D1} = \frac{3\sqrt{3}}{4} (2k_p\psi)^{1/3} \left(\frac{a_0 ct}{\sigma_\perp} \right)^{2/3}, \tag{3}$$

where $\sigma_\perp$ is the spotsize.

The transition from 1D to 3D regime occurs when Γ_{3D1} becomes larger than Γ_{1D1}. For the parameters used in our 2D simulation, this transition happens at the very beginning of the interaction, which means that ESM dominates most of the time. In 1D simulations only FRS is present.

Putting ψ to be half of the pulse length and neglecting the length of the pulse compared to the interaction length, we can rewrite Eq. (2) and Eq. (3) in the following form:

$$\Gamma_{1D1} = \quad 21 \frac{\omega_p^2}{\omega^2} \left(\frac{t}{T_R} \right)^{1/2} \left(\frac{\varepsilon[mJ]}{\lambda[\mu]} \right)^{1/2}, \tag{4}$$

$$\Gamma_{3D1} = \quad 12.5 \frac{\omega_p}{\omega} \left(\frac{t}{T_R} \right)^{2/3} \left(\frac{\varepsilon[mJ]}{\lambda[\mu]} \right)^{1/3}; \tag{5}$$

where ε is the pulse energy, λ is the laser wavelength, $T_R = \pi \sigma_\perp^2 / \lambda c$ is the Rayleigh time.

Note that Eqs. (1-5) should be applied only for qualitative estimates of the modulation amplification, because for small values of Γ the asymptotic solution is not accurate, whereas for large values of Γ other effects lead to saturation.

2.2. Relevant regime for Raman seeding

Depending on the value of Γ, the following regimes of modulation can be distinguished:

- $\Gamma \gg 1$ - the modulation quickly develops from any perturbation and saturates almost instantaneously.
- $\Gamma > 1$ - the modulation growth depends strongly on the initial perturbation.
- $\Gamma \leq 1$ - the modulation fails to develop during the interaction time regardless of initial conditions.

The intermediate regime with $\Gamma > 1$ is the main focus of this work. There are two reasons for this.

First, by introducing a finite amplitude external perturbation with Raman seed, we can reduce the energy threshold for modulation and strong wakefield excitation to the low mJ range (see Eq. (4) and Eq. (5)). Since pulsed laser systems can typically produce ~ 10 W average power, repetition rate approaching 1 kHz may be within reach. However, modulation growth and electron production depends critically on additional seeding. Second, since in this regime the seed is critical, new opportunities arise to control the phase of the generated wakefield and the rate of particle production through manipulation with the seed pulse (see section 3.1).

2.3. Raman seed amplitude

In order to determine the optimal amplitude of the seed we perform two sets of 1D PIC simulations with different ratios of seed to mail pulse amplitudes a_{0seed}/a_0. The initial total laser energy is the same in all the simulations. The initial laser pulse is split into two pulses, then the second pulse is Raman shifted in a Raman-active crystal. The first pulse and the Raman-shifted (seed) pulses are then combined and propagate in a plasma for $500\omega_p^{-1}$. Figure 1 illustrates how the maximum electron kinetic energy
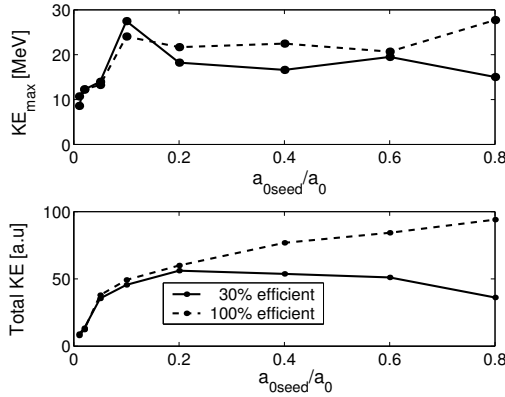
FIGURE 1. Maximum electron kinetic energy (top graph) and the total energy of relativistic ($KE > 1$ MeV) electrons (bottom graph) at $t = 100\omega_p^{-1}$ as a function of relative seed amplitude. The initial total laser energy in all the simulations is the same. The dashed curves correspond to the assumption that Raman shifting is 100% efficient. The solid curve corresponds to the assumption that the efficiency of Raman shifting is 30% in energy [20].

(KE) the total energy of relativistic (with $KE > 1$ MeV) electrons depend on the relative seed amplitude, a_{0seed}/a_0. We make following two observations. First, only a relatively small seed amplitude ($\sim 1\%$ of the intensity of the main pulse) is required to cause the onset of the modulation instability, leading to substantial particle accelerations. Second, the further increase of the seed amplitude to such a value, where the second pulse has an intensity comparable to the main pulse (beatwave regime) does not give rise to significant additional benefits if conversion loses are taken into account. The underlying reasons for that are energy losses during Raman shifting and fast degradation of the modulation structure caused by the scattering of both waves.

Experimentally, the production of a relatively large a_{0seed} comparable to a_0, for our high plasma density regime would require Raman shifting and amplification, a cumbersome and expensive proposition. For our analysis hereon, we choose $a_{0seed}/a_0 = 0.1$, which corresponds to the maximum electron energy (see Fig. 1) and is not difficult to produce in practice.

3. EFFECT OF SEED PARAMETERS ON LWFA

3.1. Coherent control with Raman seed

Controlling the phase of the wakefield is important if RS LWFA is used as an injector. Since the most energetic electrons are localized around certain phase of the plasma wave, adjusting this phase can be used to synchronize these electrons with the accelerating structure in the second stage of the acceleration.

Moreover, although in the 2D simulations presented in this work the excited plasma

wave amplitude is large enough to trap the background electrons, which have been pre-heated by BRS, lower amplitude pulses are capable of exciting plasma waves without particle trapping. Such wakefields can be used to accelerate externally injected particles or in multistage accelerators. In this regime Raman seed not only enhances the modulation but also can be used to control the phase of the excited wakefield. The simulations show that the phase of the plasma wave is equal (up to a constant) to the phase difference between the main pulse and the seed pulse, in contrast to SM-LWFA, where the modulation grows from the noise, which results in indeterminate phase with random shot-to-shot fluctuations.
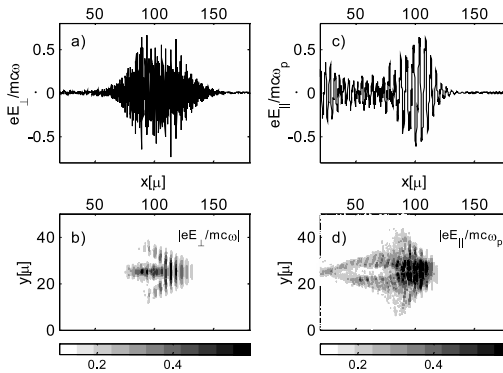

FIGURE 2. Seed, $a_0 = 0.5$, $t = 500\omega_p^{-1} = T_R$. Graphs a and b show the pulse amplitude. Graphs c and d show the wakefield.

4. 2D PIC SIMULATIONS

Experiments indicate that energetic electron production for SM-LWFA occurs only when the laser power exceeds the critical power $P > P_c$ [8]. We use 2D PIC simulations to show that the introduction of a small amplitude (1% in intensity) Raman seed enhances the modulation and leads to relativistic particle production for pulses of critical power or less. We choose a laser pulse of amplitude $a_0 = 0.5$, spot size $w = 6$ μ, wavelength $\lambda = 0.8$ μ, and duration $\tau = 125$ fs. This pulse is at critical power $P \approx P_c$ for $\omega/\omega_p = 6$ so the effects of diffraction is compensated by relativistic self-focusing. The simulation results at $t = T_R$ are given in Fig. 2. Fig. 2a shows the laser field along the beam axis. The pulse has acquired a significant modulation. Fig 2b shows that while the main pulse along the beam axis is well focused, a subpulse is developed on each side, which suggests the presence of the filamentation process. The corresponding wakefield excitation is illustrated in Fig. 2c and 2d. The wakefield along the propagation axis is shown in Fig. 2c. Notice the presence of large wakefield excitation with amplitude $\sim 0.6\omega_p mc/e$ which begins near the center of the pulse. This large wakefield is stretched out by about one-third of the pulse length. Then a wavebreak occurs which leads to the destruction of the wakefield. Figure 2d shows the wakefield excitation is trailing behind

the pulse with a "wavebreak" occurring near the beam axis behind the pulse. This is a 2D transverse wavebreaking, which leads to a significant reduction of particle energy of the accelerated electrons compared to that for the 1D case.

At $t = T_R$, the total charge of hot electrons produced is 0.62 nC, which is produced by a Raman-seeded pulse, with pulse energy equal to 38 mJ. This is to be compared to recent experimental results [8] where $\sim$ 1 nC hot electrons is generated by 500 mJ pulse.

The simulation of the same pulse without seed indicated no significant wakefield excitation or particle acceleration even for larger times.

5. CONCLUSION

Raman seeded acceleration has some distinct advantages over conventional high amplitude self-modulation accelerators. First, the resulting modulation structures and the wakefields turn out to be very clean and can be controlled by seed pulse parameters. The possibility of coherently controlling the wakefield can be especially important for beam shaping or in multistage accelerators, when the external particle injection is used. Second, our simulations indicate that a 38 mJ Raman seeded pulse can excite very strong wakefield that can trap and accelerate 0.6 nC of multi-MeV (10-20 MeV) electrons. With the conservative assumption that the laser system can sustain in average 10 W of radiated power, we conclude that acceleration is possible at $f_{rep} = 260$ Hz. By contrast, most wakefield experiments in the self-modulation regime were done with single shot $f_{rep} \ll 1$ Hz, up to the maximum repetition rate 10 Hz. High repetition rate means large average current, which is important in many applications, such as radiation oncology [11] or isotope production [8].

Our 2D simulations show that subcritical, controlled Raman-seeded wakefield excitation continues to occur at main pulse intensities even lower than the examples presented above, although, very few particles are trapped during wavebreaking. Nevertheless, external injection might be used in this regime to enable RS-LWFA at even higher repetition rates.

6. ACKNOWLEDGMENTS

REFERENCES

1. Esarey, E., Sprangle, P., Krall, J., and Ting, A., *IEEE Trans. Plasma Science*, **24**, 252–288 (1996).
2. Sprangle, P., Esarey, E., Krall, J., and Joyce, G., *Phys. Rev. Lett.*, **69**, 2200 (1992).
3. Antonsen, T. M., and Mora, P., *Phys. Rev. Lett.*, **69**, 2204–2207 (1992).

4.   Andreev, N. E., Gorbunov, L. M., Kirsanov, V. I., Pogosova, A. A., and Ramazashviki, R. R., *JETP Lett.*, **55**, 571 (1992).
5.   Najmudin, Z., Krushelnik, K., Clark, E. L., Mangles, S. P. D., Walton, B., Dangor, A. E., Fritzler, S., Malka, V., Lefebvre, E., Gordon, D., Tsung, F. S., and Joshi, C., *Phys. of Plasmas*, **10**, 2071 (2003).
6.   Malka, V., Fritzler, S., Lefebvre, E., Aleonard, M. M., Burgy, F., Chambaret, J. P., Chemin, J. F., Krushelnick, K., Malka, G., Mangles, S. P. D., Najmudin, Z., Pittman, M., Rousseau, J. P., Scheurer, J. N., Walton, B., and Dangor, A. E., *Science*, **298**, 1596 (2002).
7.   Wagner, R., Chen, S. Y., Maksimchuk, A., and Umstadter, D., *Phys. Rev. Lett.*, **78**, 3125–3128 (1997).
8.   Leemans, W. P., Rodgers, D., Catravas, P. E., Geddes, C. G. R., Fubiani, G., Esarey, E., Shadwick, B. A., Donahue, R., and Smith, A., *Phys. Plasmas*, **8**, 2510–2516 (2001).
9.   Krishnan, S. Y. C. M., Maksimchuk, A., Wagner, R., and Umstadter, D., *Phys. Plasmas*, **6**, 4739–4749 (1999).
10. Tajima, T., *J. Jpn. Soc. Therap. Rad. Oncol.*, **9**, 83 (1997).
11. Chiu, C., Fomytskyi, M., Grigsby, F., Raischel, F., Downer, M., and Tajima, T., *Med. Phys.*, **31**, 2042 (2004).
12. Kainz, K. K., Hogstrom, K. R., Antolak, J. A., Almond, P. R., Bloch, C. D., Chiu, C., Fomytskyi, M., Raischel, F., Downer, M., and Tajima, T., *Med. Phys.*, **31**, 2053 (2004).
13. Modena, A., Najmudin, Z., Dangor, A. E., Clayton, C. E., Marsh, K. A., Joshi, C., Malka, V., Carrow, C. B., Danson, C., Neely, D., and Walsh, F. N., *Nature (London)*, **377**, 606 (1995).
14. Ting, A., Moore, C. I., Krushelnik, K., Manka, C., Esarey, E., Sprangle, P., Hubbard, R., Burris, H. R., Fischer, R., and Baine, M., *Phys. Plasmas*, **4**, 1889 (1997).
15. Malka, G., Lefebvre, E., and Miquel, J. L., *Phys. Rev. Lett.*, **78**, 3314 (1997).
16. Bagnoud, V., and Salin, F., *Appl. Phys.*, pp. S165–S170 (2000).
17. Fomytskyi, M., Chiu, C., Downer, M., and Grigsby, F., Raman-seeded laser wakefield acceleration (2004), submitted to Phys. Plasmas.
18. Andreev, N. E., Gorbunov, L. M., and Kirsanov, V. I., *Plasmas Phys. Rep.*, **21**, 872–883 (1995).
19. Fisher, D. L., and Tajima, T., *Phys. Rev. E*, **53**, 1844–1851 (1996).
20. Zhavoronkov, N., Noack, F., Petrov, V., Kalosha, V. P., and Jerrmann, J., *Opt. Lett.*, **26**, 47–49 (2001).
21. Andreev, N. E., Gorbunovand, L. M., Kirsanov, V. I., Pogosova, A. A., and Sakharov, A. S., *Plasmas Phys. Rep.*, **22**, 419–430 (1996).
22. Mori, W. B., *IEEE J. Quant. Elec.*, **33**, 1942–953 (1997).
23. Decker, C. D., Mori, W. B., and Katsouleas, T., *Phys. Plasma*, **3**, 1360 (1996).